A molecular perspective on the cleaning of oil paintings

Baij, C.L.M.

Publication date
2020
Document Version
Other version
License
Other

CHAPTER

FOUR

THE CONCENTRATION AND ORIGINS OF CARBOXYLIC ACID GROUPS IN OIL PAINT

Parts of this chapter are published in:

L. Baij, L. Chassouant, J. J. Hermans, K. Keune and P. D. Iedema, The concentration and origins of carboxylic acid groups in oil paint, *RSC Advances*, **2019**, 9, 35559–35564.

4.1 Introduction

The degradation of oil paintings manifests itself by visible and mechanical paint alterations such as brittleness, loss of opacity, formation of protrusions, and delamination of paint layers.[3] These alarming phenomena have initiated the chemical analyses of many paint samples over the past decades. However, thorough understanding of the underlying chemical and physical mechanisms causing paint degradation started only recently.[29,42,43,102,109] The chemical composition of a mature oil paint binder has proved to play an essential role in several of these degradation phenomena. Understanding the driving forces behind degradation processes will ultimately provide useful knowledge for the preservation and conservation of oil paintings.

We have shown previously that in a mature oil paint binding medium, carboxylic acid (COOH) groups often bind to metal ions (originating from pigments or driers) and form an ionomeric polymer network.[42,43] The ionomeric binding medium, like commercial ionomers,[110] contains clusters of metal carboxylates (COOM), often identified by a broad asymmetric ν_a COO^- infrared (IR) absorption band.[43,109] These ionomeric metal carboxylate complexes were discovered to represent an intermediate stage in paint ageing that can ultimately lead to the appearance of crystalline metal soaps (metal complexes of long chain saturated fatty acids).[29] Metal soaps play an important role in many types of oil paint degradation.[3]

The concentration of COOH groups in polymerised oil is expected to be a crucial factor affecting the extent of oil paint degradation. Being an integral part of the mature oil paint binding medium, COOH groups are most likely the driving force for the release of metal ions by inorganic pigments and the formation of (network-bound) COOM.[43] Furthermore, COOH groups indirectly determine the extent of metal soap formation, because before metal soap crystallisation can occur, network-bound COOM need to exchange with free SFAs.[29] Although many[13,14,111–117] have studied *extractable* acids, the concentration of COOH groups linked to the polymer network has, to the best of our knowledge, never been quantified.

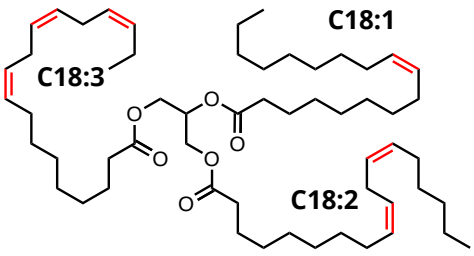

Figure 4.1 Structure of a triacylglyceride (TAG) unit in linseed oil (LO), C18:3 denotes linolenic acid, C18:2 linoleic acid and C18:1 oleic acid.

From a chemical point of view, oil paint is a mixture of mainly inorganic pigments, a drying oil consisting of triacylglycerides (TAGs) and a variety of possible additives. Linseed oil (LO) is widely used in oil paintings because it possesses excellent drying properties. LO consists of a mixture of TAGs, mostly containing linolenic acid (C18:3), linoleic acid (C18:2), and oleic acid (C18:1) side chains (see Figure 4.1). As the oil undergoes autoxidation reactions,[4–6] the paint mixture becomes a complex heterogeneous polymer with solid pigment particles suspended in the densely cross-linked network. This polymer network contains mainly ether- or peroxy-type cross-links formed through autoxidation of double bonds on fatty acid side chains. Over time, higher oxidation products of these oxygen cross-links result in the formation of aldehydes and COOH groups (see Scheme 4.1). It is important to note that COOH groups are a product of the autoxidation process (mechanism 2). Consequently, the ionomeric state is also found in relatively young oil paints. Upon ageing, hydrolysis of ester bonds can introduce additional COOH groups (mechanism 1). Since the two different mechanisms of COOH formation may dominate at different stages during the lifetime of an oil paint, we aim to distinguish them in our experiments.

The present chapter focuses on the crucial role COOH groups play in pigment degradation. Quantifying the amount of COOH groups attached to a heterogeneous polymer network is a challenging task. Most spectroscopic, electrochemical or calorimetric methods to determine the acid concentration in vegetable oils require a homogeneous solution of the (non-polymerised) oil in a solvent and only work for free fatty acids (FFAs).[118,119] Because we are interested in the COOH groups linked to the polymer network, the conventional methods of breaking up TAGs using pyrolysis GC/MS do not give the desired information.[120] Potentiometric titration of COOH groups[121] proved to be time consuming and inaccurate since polymerised LO is extremely insoluble and the diffusion of water is very slow.[122] Methods based on derivatisation with fluoride transfer reagents[38,123] showed the existence of acid groups but did not give a reproducible conversion when applied to our polymeric materials. Swollen-state ^{13}C NMR spectroscopy also enabled the detection of acid groups but was not used in a quantitative manner.[124]

Attenuated total reflection Fourier-transform infrared (ATR-FTIR) spectroscopy is a powerful tool for the study of organic polymers and solid paint materials. However, ATR-FTIR does not allow for a direct observation of the COOH concentration in polymerised LO due to the overlapping IR absorption bands of the asymmetric carbonyl stretching vibration of the ester (COOR, 1738 cm^{-1}), aldehyde (COH, 1726 cm^{-1}) and carboxylic acid (COOH, 1710 cm^{-1}) groups (see Figure A.1). Simple peak deconvolution is unreliable because additional overlapping absorption contributions from FFAs, ketones and ν(C=C) bonds are present in this spectral region.[125] A practical solution is the complexation of COOH groups with Zn^{2+} ions (released by ZnO), leading to the appearance of a broad, free-lying IR absorption band for zinc carboxylates (COOZn) centered around 1585 cm^{-1}.[42,109] We have recently unequivocally assigned the structure and coordination in these COOZn

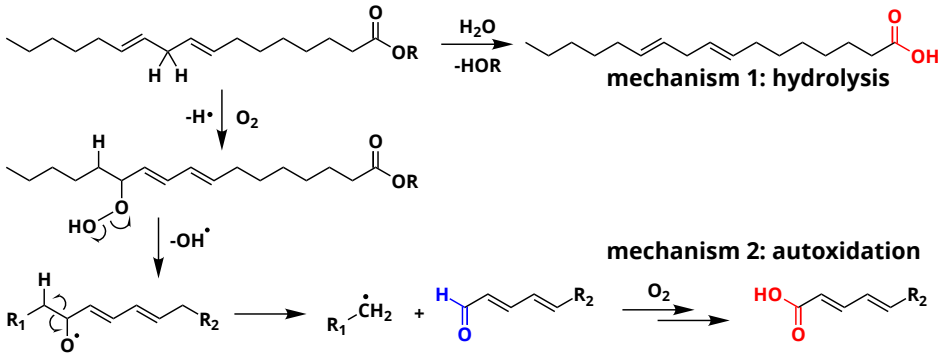

Scheme 4.1 Two mechanisms that lead to the formation of acid groups (in red) starting from the ester of linoleic acid: (1) hydrolysis and (2) autoxidation of side chain C=C bonds. Note that autoxidation leads to additional products, including aldehydes (in blue).

complexes: they adopt either a coordination chain- or an oxo-type cluster structure (see CHAPTER 5).[109] The COOZn IR absorption band can be used as a method to accurately estimate the concentration of COOH in polymerised LO that is accessible for reaction with zinc ions. This concentration is most relevant for oil paint degradation since amorphous COOZn is the intermediate in crystalline metal soap formation. Throughout this text, the COOZn band will be used as a measure for COOH concentration.

In our experiments, we monitor COOZn formation by varying the amounts of ZnO or COOH in a controlled manner. In one series of experiments, the ZnO concentration is increased at constant COOH concentration. In a second series of experiments, the acidity is varied under excess ZnO. Because acid groups in polymerised LO can form according to two mechanisms: (1) hydrolysis of ester bonds and (2) autoxidation of side chains double bonds (see Scheme 4.1), we also investigate which mechanism of COOH group formation dominates. Regular LO does not allow to discriminate between these two mechanisms of acid formation. We employ a mixture of alcohols obtained by reducing LO with $LiAlH_4$, blocking the hydrolysis pathway and forming acid groups by autoxidation only. Because the concentration of acid groups in our model systems is not universally valid for aged paintings, we investigate how environmental conditions affect the COOH concentration. More specifically, the influence of ZnO on ester hydrolysis is investigated by examining samples at low and high relative humidity (RH) as a function of ZnO concentration.

In this chapter, we develop an analytical method to quantify the concentration of COOH groups attached to a complex polymerised oil network. Knowing the quantity and origins of COOH groups can lead to improved storage and conservation strategies and an extended lifetime of invaluable works of art.

4.2 Results and Discussion

4.2.1 COOH concentration in ZnO paints

Paints with increasing ZnO content To explore the effect of ZnO concentration on COOZn formation, mixed pigment paint models containing various amounts of ZnO and a $BaSO_4$ filler were prepared (denoted **LO-ZnO-BaSO$_4$**). The $BaSO_4$ pigment is a well-known inert filler[126] for white paints with a comparable density to ZnO (ZnO and $BaSO_4$: 5.6 and 4.5 g/cm^3, respectively). Within the series, the total PVC was kept constant. The exact sample composition is given in Table A.1.

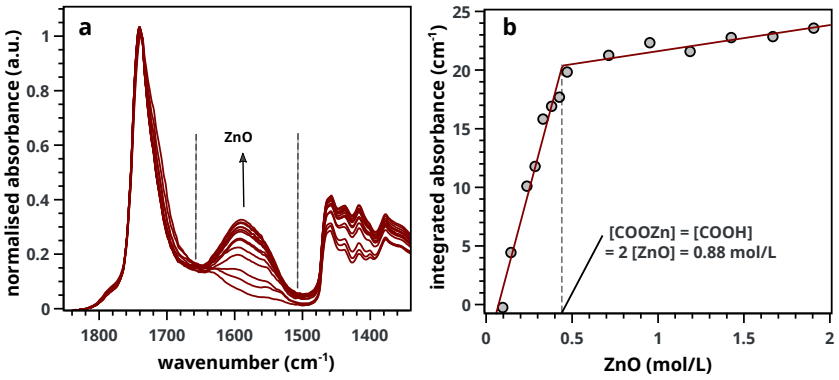

Figure 4.2 **a**: Ester normalised ATR-FTIR spectra for **LO-ZnO-BaSO$_4$** from 0.14–1.8 mol/L of added SA (0.0–20 wt%). Dashed lines indicate band integration limits. **b**: Integrated absorption values of COOZn band, clearly showing the 'tipping point' (dashed line) at 0.44 mol/L ZnO marking complete COOH neutralisation. Further increase of ZnO does not increase the amount of COOZn. See Figure 4.7 for details on spectral processing.

Ester normalised FTIR spectra for samples containing 0.5–20 wt % of ZnO are depicted in Figure 4.2a, showing an increasing concentration of COOZn with increasing ZnO content. Integrated absorption values for the ν_a COOZn IR absorption band at 1585 cm^{-1} are plotted as a function of ZnO concentration in Figure 4.2b. Two regimes are visible in Figure 4.2b, separated by a clear 'tipping point': a steep increase in COOZn up to 0.44 mol/L ZnO in LO ($\approx$ 4.5 wt% of ZnO) and a minimal increase in COOZn at concentration above 0.44 mol/L. These results indicate that below 0.44 mol/L ZnO, part of the acid groups are complexated with zinc ions but there is insufficient ZnO present to neutralise all acid groups. The complete conversion of ZnO below 0.44 mol/L was confirmed by XRD (see Figure A.5). Above 0.44 mol/L, an excess ZnO is present and all accessible acid groups are complexated with zinc. Consequently, the tipping point can be used to calculate the concentration of COOH group available for reaction with ZnO: at this point the concentration of COOH is equivalent to twice the concentration of COOZn (and thus ZnO). This approach leads to a calculated [COOH] of 0.88 mol/L and

a molar [COOH]/[COOR] ratio of 0.35. This result means that for roughly every three COOR functionalities, one COOH group is formed. In absence of ester hydrolysis, this corresponds to about one COOH group per triacyglycerol (TAG) unit or LO molecule.

Standard addition of sorbic acid To test if additional acid groups in the linseed oil binder would result in the formation of additional COOZn, paints with increasing acidity were synthesised by cross-linking sorbic acid (SA, 2,4-hexadienoate) into ZnO based paint model systems (**LO-ZnO-SA**). Using the standard addition method, these experiments form a second method of COOH quantification. A constant PVC with a ZnO to LO ratio of 1:1 (w/w) was used in this experiment, ensuring an large excess of ZnO.

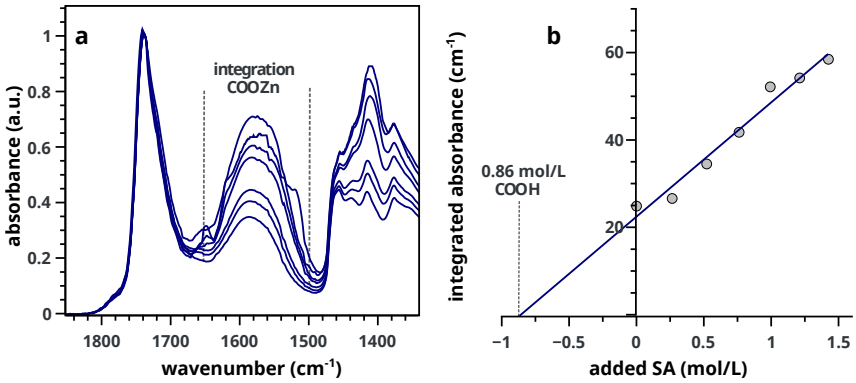

Figure 4.3 **a**: selection of FTIR spectra of **LO-ZnO-SA** with added SA from 0.0–1.5 mol/L of ZnO in LO (0–60 wt%). Dashed lines in indicate band integration limits. **b**: Integrated absorption values of COOZn band showing the linear relationship between added SA and COOZn absorption.

The effect of functionalising LO with additional acid groups on the COOZn IR absorption band at 1585 cm^{-1} is shown in Figure 4.3**a**. Integrated absorption values of the COOZn band are plotted as a function of added SA in Figure 4.3**b**. Evidently, there is a linear (R^2 = 0.97) relationship between the concentration of acid groups and the COOZn band, confirming the tendency of these systems to form COOZn as long as a source of zinc (ZnO) is present. The concentration of acid groups in pure **ZnO-LO** (without SA) was calculated to be 0.86 mol/L, resulting in a [COOH]/[COOR] ratio of 0.32 (Figure 4.3**b**). This result is in excellent agreement with our previous result obtained with mixed ZnO/$BaSO_4$ paints.

4.2.2 The origin of COOH formation

Having established a method to determine the COOH concentration in our paint samples, we proceed to investigate whether these acid groups originate from autoxidation of side

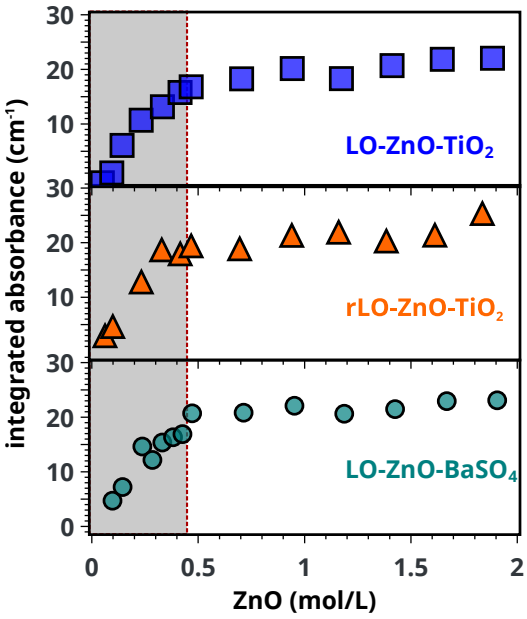

Figure 4.4 Integrated absorbance of the COOZn band for **LO-ZnO-TiO_2**, **rLO-ZnO-TiO_2** and **LO-ZnO-$BaSO_4$** model systems. The dotted line indicates the previously found tipping point at 0.44 mol/L ZnO. All IR spectra were normalised on the CH_2 stretching vibration (2929 cm^{-1}) before integration.

chain double bonds or from the hydrolysis of ester carbonyl functionalities. Effects of increasing RH and ZnO concentration on COOZn formation are investigated.

Autoxidation The relative amount of autoxidation and the effect of ZnO concentration on COOZn formation was studied. A mixture of alcohols obtained by reducing the esters in linseed oil to alcohols (reduced LO, **rLO**) was used as a binding medium instead of LO. This approach ensures that all COOZn formation results from autoxidation. Model paint samples containing **rLO** with varying amounts of ZnO and TiO_2 fillers (**rLO-ZnO-TiO_2**) were made. Coated rutile TiO_2 fillers were selected for the highly inert properties and low photocatalytic activity.[127] In order to compare the two mechanisms of COOH formation (Scheme 4.1), reduced LO containing model paints were compared with samples made with ordinary LO.

Comparing **rLO-ZnO-TiO_2** (triangles) with **LO-ZnO-TiO_2** (squares) in Figure 4.4, it is clear that using **rLO** does not significantly affect COOZn formation at low ZnO concentrations (0.1–2 mol/L). Hence, we conclude that the previously calculated COOH concentration of 0.88 mol/L is the result of side chain autoxidation (Scheme 4.1, pathway 2). Figure 4.4 also shows that the integrated absorption values of the COOZn band in **LO-ZnO-$BaSO_4$** (circles) and **LO-ZnO-TiO_2** (squares) are highly similar, verifying the chemical inertness of the chosen TiO_2 and $BaSO_4$ fillers. To confirm that autoxidation is

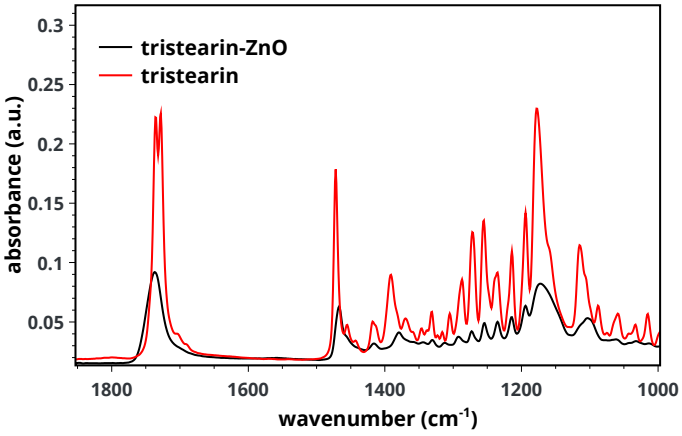

Figure 4.5 FTIR spectrum of tristearin and tristearin-ZnO, clearly showing that 1 week at 60°C and 12% RH did not lead to the formation of significant amounts of COOZn. A split ester carbonyl band is observed for tristearin due to the presence of different polymorphs.[128,129]

the main pathway leading to the formation of COOH groups in **rLO-ZnO-TiO$_2$** samples, we cured a mixture of fully saturated triglycerides (tristearin) and ZnO (1:1 by wt.) for one week at 60 °C and 12% RH. In this mixture, no COOZn was formed after one week (see Figure 4.5).

Hydrolysis Having established that autoxidation is dominant at low RH, we investigated high RH conditions and increasing ZnO concentrations because these factors likely promote ester hydrolysis. A number of recent publications have already demonstrated the relationship between the presence of ZnO[14] or high RH conditions and the formation of organic acids in paint extracts.[116,117] We compared **LO-ZnO-TiO$_2$** and **rLO-ZnO-TiO$_2$** paint models cured in dry (12% RH) and wet conditions (77% RH). A large ZnO concentration range of 3–9 mol/L (30–90 wt% of ZnO in LO) was studied.

Integrated absorbance values of the COOZn band at 1585 cm^{-1} for **LO-ZnO-TiO$_2$** and **rLO-ZnO-TiO$_2$** cured in dry and wet conditions are plotted as a function of ZnO concentration in Figure 4.6. The integrated COOZn absorbance for both systems cured in 77% RH conditions is significantly higher than when cured at 12% RH (Figure 4.6). Interestingly, both **LO-ZnO-TiO$_2$** and **rLO-ZnO-TiO$_2$** show this effect, indicating that autoxidation is also the dominant pathway for COOH formation at high RH conditions and high ZnO concentrations. Previous research has shown that the oxygen uptake and peroxide decomposition rate in methyl linoleate are, in the first 80 hours, lower at higher water activities, resulting in a lower quantity of carbonyl compounds.[130] Upon longer autoxidation times of up to two weeks, the production rates of hydroperoxides and conjugated dienoic acids were found to increase with increasing water activities.[131] Water can thus stabilise and destabilise intermediates during different stages of the autoxidation pathway, resulting in

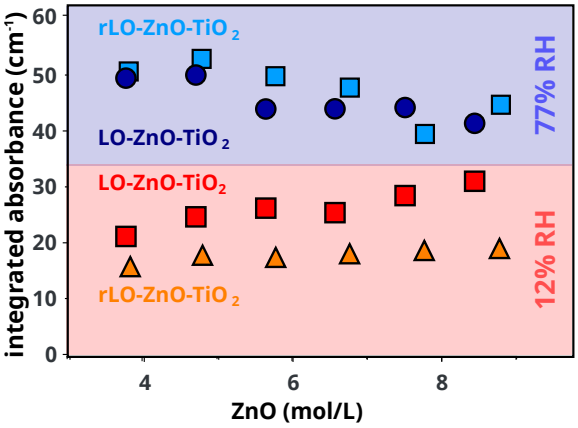

Figure 4.6 Integrated absorbance of the COOZn band for **LO-ZnO-TiO_2** and **rLO-ZnO-TiO_2** from 30%–90 wt% cured in 12% and 77% RH at 60 °C for 7 days. All IR spectra were normalised on the CH_2 stretching vibration (2929 cm^{-1}) before integration.

an increased formation of COOH groups for long oxidation times. This can explain the increased COOZn formation at 77% RH conditions in our measurements.

Comparing both systems at 12% RH, a small but significant difference is visible: the integrated absorbance for the COOZn band is consistently larger for **LO-ZnO-TiO_2** and seems to increase with increasing ZnO concentration. It is known that the low concentrations of free FAs (0.5 wt%) can significantly increase the rate of autoxidation in methyl linoleate.[132] The presence of free FAs in the regular LO may thus explain the formation of more COOZn in **LO-ZnO-TiO_2**. This effect is not visible at 77% RH, suggesting that the effects of water on autoxidation are stronger than the effects of free FAs at high humidity. We currently do not have a satisfying explanation for the increase in COOZn with increasing ZnO at 12% RH for **LO-ZnO-TiO_2**. Since we have shown that there is no hydrolysis of ester bonds in a mixture of ZnO and tristearine at 12% RH, hydrolysis can not explain this effect.

4.3 Conclusions

The concentration of acid groups in analytically challenging polymerised oil paint models was quantified using ATR-FTIR. Because the formation of COOH groups drives the release of zinc ions from ZnO pigment to form COOZn, this mechanism can be used to determine the concentration of COOH groups available for coordination with zinc ions. The COOH concentration in ZnO paint models was calculated to be roughly one COOH group per TAG unit. This result was confirmed using the standard addition of sorbic acid to linseed oil in excess of ZnO.

At low ZnO concentrations and low RH, COOH groups were found to form by au-

toxidation only. To investigate conditions that likely promote ester hydrolysis, the effects of moisture on COOH formation were studied over a wide range of ZnO concentrations. A strong increase in COOZn was observed at 77% RH compared to 12% RH due to an accelerating effect of water on COOH formation. No hydrolysis was observed under the conditions studied, indicating that oil paints are, in the initial stage of curing, quite resistant to hydrolysis.

Our results demonstrate that smart design of models systems enable a better understanding of oil paint degradation, aiding the improvement of storage and conservation strategies.

4.4 Experimental

ATR-FTIR spectroscopy ATR-FTIR spectra were measured on a Perkin-Elmer Frontier FT-IR spectrometer fitted with a Pike GladiATR module equipped with a heated top plate and a diamond ATR-crystal ($\varnothing$ = 3 mm). Spectra were averaged over 4 scans. To integrate overlapping absorption bands, automated data correction and integration algorithms were written using Wolfram Mathematica software. For integration, IR spectra were averaged over either 3 or 5 measurements and the baseline was set to zero at 1820 cm^{-1}. Spectra were normalised on the ester carbonyl (1740 cm^{-1}) or CH_2 (2920 cm^{-1}) band, after which the ester CO band was subtracted and integration performed between 1500–1650 cm^{-1}. An estimated non-linear baseline correction was used to remove TiO_2 absorption. An illustration of the background subtraction and band fitting procedures is given in Figure 4.7 and Figure 4.8. In all graphs, error bars due to spectral variation are smaller than the symbols.

To integrate overlapping absorption bands accurately, data correction and integration algorithms were written in the Wolfram *Mathematica* software, which are available from the authors on request. Since the zinc carboxylate (COOZn) band present in ZnO-LO samples at 1585 cm^{-1} overlaps with the ester carbonyl band (maximum at 1738 cm^{-1}), a band fitting algorithm was applied to subtract the ester band and integrate the COO-Zn band accurately (see Figure 4.7a). After subtraction of the Pearson type IV band shape[108] fitted to the ester carbonyl band, the area of the COOZn band was calculated (Figure 4.7b, integration limits are indicated with a dashed line).

Sample preparation Model paint samples containing ZnO (Sigma Aldrich, $\geq$99%) and coated rutile TiO_2 (Sigma Aldrich, >99.9%) or ZnO and $BaSO_4$ (Kremer pigmente 58700, $\geq$98%) were made by grinding the pigments with cold-pressed untreated linseed oil (Kremer pigmente) in a 1:1 (w/w) ratio to a smooth paste with mortar and pestle. SEM images of pigment particles are shown in Figure A.4. The successful reduction of the esters in LO to alcohols was achieved using $LiAlH_4$ in tetrahydrofuran (THF) (see next paragraph and Figure A.2). Care was taken to keep the Pigment Volume Concentration

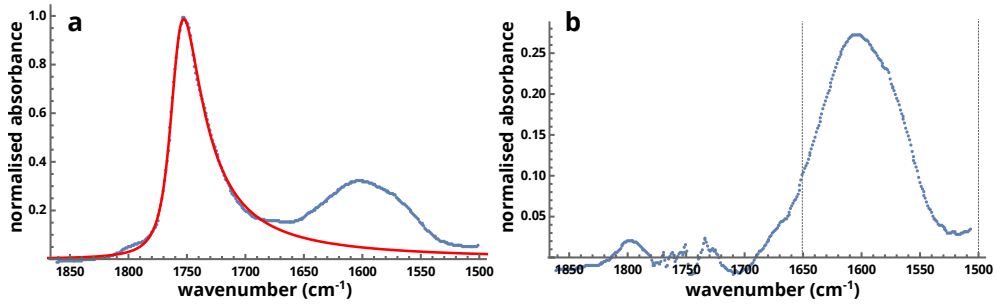

Figure 4.7 Subtraction procedure for the asymmetric stretching vibration (ν_a CO) of the ester (COOR, 1738 cm^{-1}) in polymerised LO. **a**: A Pearson type IV band shape[108] was fitted to the experimental data and **b** subtracted before integration.

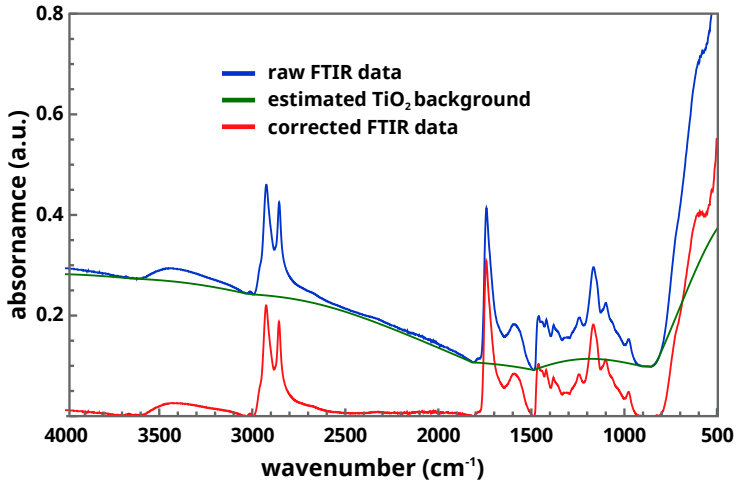

Figure 4.8 Automated background subtraction procedure using *Mathematica* software. The changing concentration of TiO_2 along the LO-ZnO-TiO_2 samples requires a different background subtraction for every sample. After TiO_2 background estimation, the COOZn band area was calculated according to Figure 4.7.

(PVC) at 17–19% in all series. The mixture was applied to 50 × 75 mm glass slides and spread with a draw-down bar to achieve a wet thickness of 190 μm. The samples were cured in the dark in air at 60 °C for 7 days at different RH. RH was controlled using a saturated NaCl solution (for 77% RH) in a closed container and was determined using a Rotronic HL-1D temperature and humidity data logger. For all measurements, 5 × 5 mm squares of the films were cut and lifted off the glass support for ATR-FTIR analysis. The exact sample composition is given in Table A.1–Table A.6.

Reduction of linseed oil with $LiAlH_4$ The reduction of linseed oil with lithium aluminium hydride $LiAlH_4$ was done according to slightly modified literature[133,134] proce-

dures. $LiAlH_4$ (5.2 g, 138 mmol) was dispersed in 225 ml cold THF (0 °C) under nitrogen atmosphere. Cold-pressed untreated linseed oil (LO, Kremer Pigmente, 15 g, 17 mmol) was added while stirring the reaction in a ice bath. The reaction mixture was then stirred continuously at allowed to reach room temperature. After 17 h, the mixture was cooled again to 0 °C and 40 ml of 2-propanol, ethanol and 20 ml of water was *slowly* added. The mixture was stirred for 15 min and filtered using a Büchner funnel. The solvent was removed *in vacuo* and the filtrate dissolved in dichloromethane and filtered over $MgSO_4$. The solvent was removed *in vacuo* to give the mixture of alcohols (14 g, 93% yield). ^{1}H NMR (300 MHz, $CDCl_3$) δ 5.50–5.21 (m, -CH=CH-), 3.64 (t, $J = 6.6$ Hz, $-CH_2OH$), 2.81 (t, J = 5.8 Hz, $-CH{=}CHCH_2CH{=}CH-$), 2.17–1.96 (m, $CH{=}CHCH_2C^-$), 1.56 (s, $-CH_2CH_2OH$), 1.37–1.28 (br, $-CCH_2C-$), 0.97 (t, $J = 7.5$ Hz, CH_3).

X-ray diffraction X-ray diffraction (XRD) measurements on cured films were recorded with a Rigaku MiniFlex II desktop X-ray diffractometer using Cu Kα radiation at 2.5°/min on ca. 10 × 10 mm squares of paint film taped to a glass sample holder.

Acknowledgements

Louise Chassouant (MSc. student, University of Amsterdam) is thanked for her great contributions to this chapter.

4.A Appendix

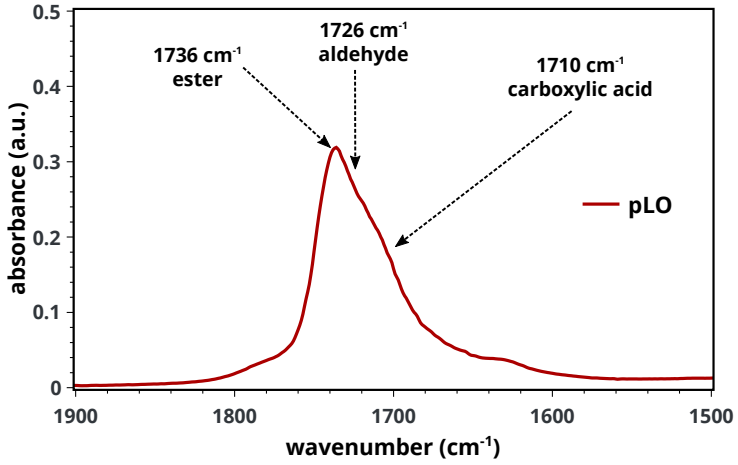

Figure A.1 Overlapping IR absorption bands of the asymmetric stretching vibration (ν_a COO) of the ester (COOR, 1738 cm^{-1}), aldehyde (COH, 1726 cm^{-1}) and carboxylic acid (COOH, 1710 cm^{-1}) carbonyl function in polymerised LO (**pLO**).

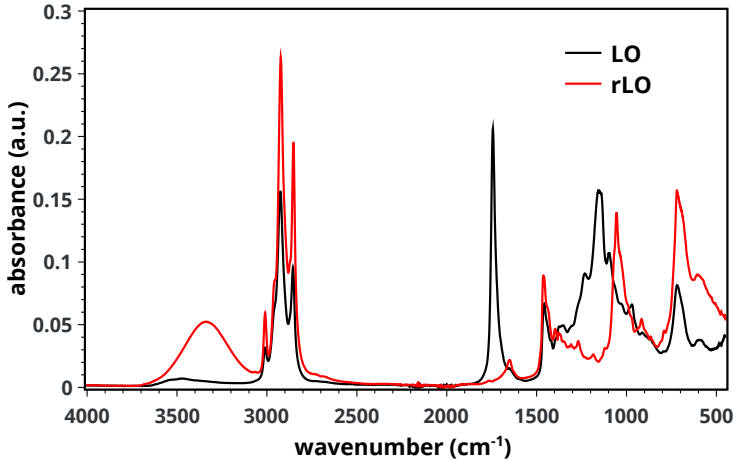

Figure A.2 FTIR spectrum of LO and reduced LO (**rLO**), clearly showing the reduction of all esters (1736 cm^{-1}) for **rLO** and the presence of the OH stretch (3400 cm^{-1}, broad) in the mixture of alcohols.

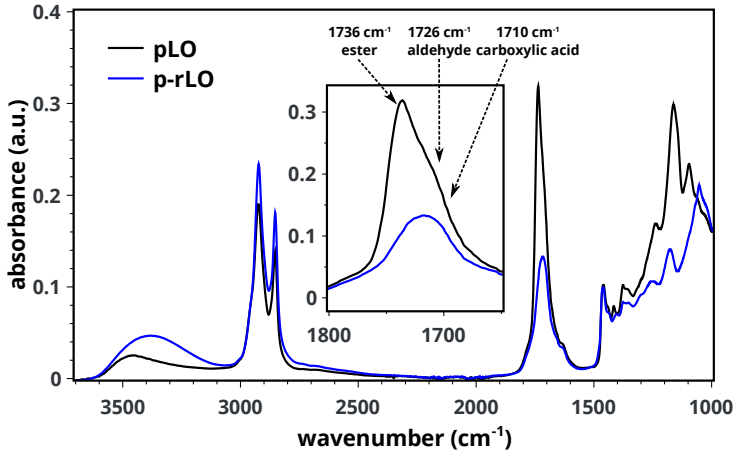

Figure A.3 FTIR spectrum of polymerised LO (**pLO**) and polymerised reduced LO (**p-rLO**).

Table A.1 Composition of LO-ZnO-$BaSO_4$ series 0.5–20% with a constant (1:1) pigment to oil ratio by weight and a PVC of 17–18%.

Sample	LO (mg)	ZnO (mg)	$BaSO_4$ (mg)	[ZnO] mol/L
LO-ZnO-$BaSo_4$-0.5	1000.2	4.80	995.0	0.045
LO-ZnO-$BaSo_4$-1	1000.1	10.2	989.7	0.097
LO-ZnO-$BaSo_4$-1.5	1000.6	15.2	985.2	0.14
LO-ZnO-$BaSo_4$-2.5	1000.3	25.0	975.2	0.24
LO-ZnO-$BaSo_4$-3	1000.3	30.1	970.0	0.28
LO-ZnO-$BaSo_4$-3.5	999.70	34.9	965.1	0.33
LO-ZnO-$BaSo_4$-4	1000.4	40.2	960.1	0.38
LO-ZnO-$BaSo_4$-4.5	999.50	44.9	955.0	0.43
LO-ZnO-$BaSo_4$-5	999.30	49.8	950.0	0.47
LO-ZnO-$BaSo_4$-7.5	999.80	75.1	924.9	0.71
LO-ZnO-$BaSo_4$-10	1000.5	100.3	900.4	0.95
LO-ZnO-$BaSo_4$-12.5	999.70	124.8	874.8	1.2
LO-ZnO-$BaSo_4$-15	1000.2	149.9	850.4	1.4
LO-ZnO-$BaSo_4$-17.5	999.80	175.2	824.9	1.7
LO-ZnO-$BaSo_4$-20	1000.2	200.0	799.7	1.9

Table A.2 Composition of LO-ZnO-TiO_2 series 0.5–20% with a with a constant (1:1) pigment to oil ratio by weight and a PVC of of 17–18%.

Sample	LO (g)	ZnO (g)	TiO_2 (g)	[ZnO] mol/L
LO-ZnO-TiO_2-0.5	999.8	5.2	994.7	0.049
LO-ZnO-TiO_2-1	1000.3	9.9	990.1	0.092
LO-ZnO-TiO_2-1.5	1000.3	15.1	985.0	0.14
LO-ZnO-TiO_2-2.5	1033.2	25.0	975.1	0.23
LO-ZnO-TiO_2-3.5	1033.2	35.3	965.0	0.33
LO-ZnO-TiO_2-4.5	1033.2	44.2	955.0	0.41
LO-ZnO-TiO_2-5	999.6	49.8	950.3	0.47
LO-ZnO-TiO_2-7.5	999.4	75.0	925.2	0.70
LO-ZnO-TiO_2-10	1000.3	100.3	900.0	0.94
LO-ZnO-TiO_2-12.5	1000.2	124.8	874.9	1.2
LO-ZnO-TiO_2-15	999.9	149.9	850.0	1.4
LO-ZnO-TiO_2-17.5	1000.6	174.9	825.1	1.6
LO-ZnO-TiO_2-20	1000.1	200.3	800.1	1.9

Table A.3 Composition of rLO-ZnO-TiO_2 series 0.5–20% with a PVC of of 17–19%

Sample	LO (mg)	ZnO (mg)	TiO_2 (mg)	[ZnO] mol/L
rLO-ZnO-TiO_2-0.5	199.5	1.3	198.4	0.059
rLO-ZnO-TiO_2-1	200.4	2.1	197.8	0.10
rLO-ZnO-TiO_2-1.5	666.4	10.0	646.3	0.14
rLO-ZnO-TiO_2-2.5	500.2	12.4	483.8	0.23
rLO-ZnO-TiO_2-3.5	500.1	17.5	481.7	0.33
rLO-ZnO-TiO_2-4.5	333.4	14.8	321.7	0.41
rLO-ZnO-TiO_2-5	332.8	16.6	321.5	0.47
rLO-ZnO-TiO_2-7.5	333.3	24.8	319.6	0.69
rLO-ZnO-TiO_2-10	251.4	25.4	239.8	0.94
rLO-ZnO-TiO_2-12.5	250.2	31.3	238.4	1.2
rLO-ZnO-TiO_2-15	200.7	30.1	191.0	1.4
rLO-ZnO-TiO_2-17.5	200.1	35.0	190.2	1.6
rLO-ZnO-TiO_2-20	200.7	40.1	189.4	1.8

Table A.4 Composition of sorbic acid (LO-ZnO-SA) series 0–60% with a constant (1:1) pigment to oil ratio by weight.

Sample	LO (mg)	ZnO (mg)	SA (mg)	[SA] mol/L
LO-ZnO-SA-0	1033.2	1006.1	0	0
LO-ZnO-SA-10	1004.1	998.3	38.3	0.26
LO-ZnO-SA-20	1000.7	999.4	77.1	0.52
LO-ZnO-SA-30	999.4	1000.0	115.2	0.76
LO-ZnO-SA-40	1000.5	1000.2	153.8	0.99
LO-ZnO-SA-50	1000.6	1000.7	192.1	1.2
LO-ZnO-SA-60	999.7	1000.5	230.9	1.4

Table A.5 Composition of LO-ZnO-TiO_2 series 30–90% with a constant PVC of 18%.

Sample	LO (mg)	ZnO (mg)	TiO_2 (mg)	[ZnO] mol/L
LO-ZnO-TiO_2-30	1000.4	302.1	753.7	2.83
LO-ZnO-TiO_2-40	1000.2	401.3	682.0	3.76
LO-ZnO-TiO_2-50	1002.2	501.1	605.0	4.69
LO-ZnO-TiO_2-60	998.90	601.1	530.9	5.64
LO-ZnO-TiO_2-70	1000.6	703.1	457.9	6.59
LO-ZnO-TiO_2-80	1005.1	800.1	381.0	7.47
LO-ZnO-TiO_2-90	1001.1	902.2	308.0	8.45

Table A.6 Composition of rLO-ZnO-TiO_2 series 30–90%. Pigment volume concentration 14–18%.

Sample	LO (mg)	ZnO (mg)	TiO_2 (mg)	[ZnO] mol/L
rLO-ZnO-TiO_2-30	201.3	59.9	139.9	0.14
rLO-ZnO-TiO_2-40	201.2	78.7	120.2	0.23
rLO-ZnO-TiO_2-50	201.4	100.3	101.5	0.33
rLO-ZnO-TiO_2-60	201.0	120.1	81.0	0.41
rLO-ZnO-TiO_2-70	201.5	139.7	59.5	0.47
rLO-ZnO-TiO_2-80	199.7	159.0	40.3	0.70
rLO-ZnO-TiO_2-90	201.5	180.5	21.1	0.94

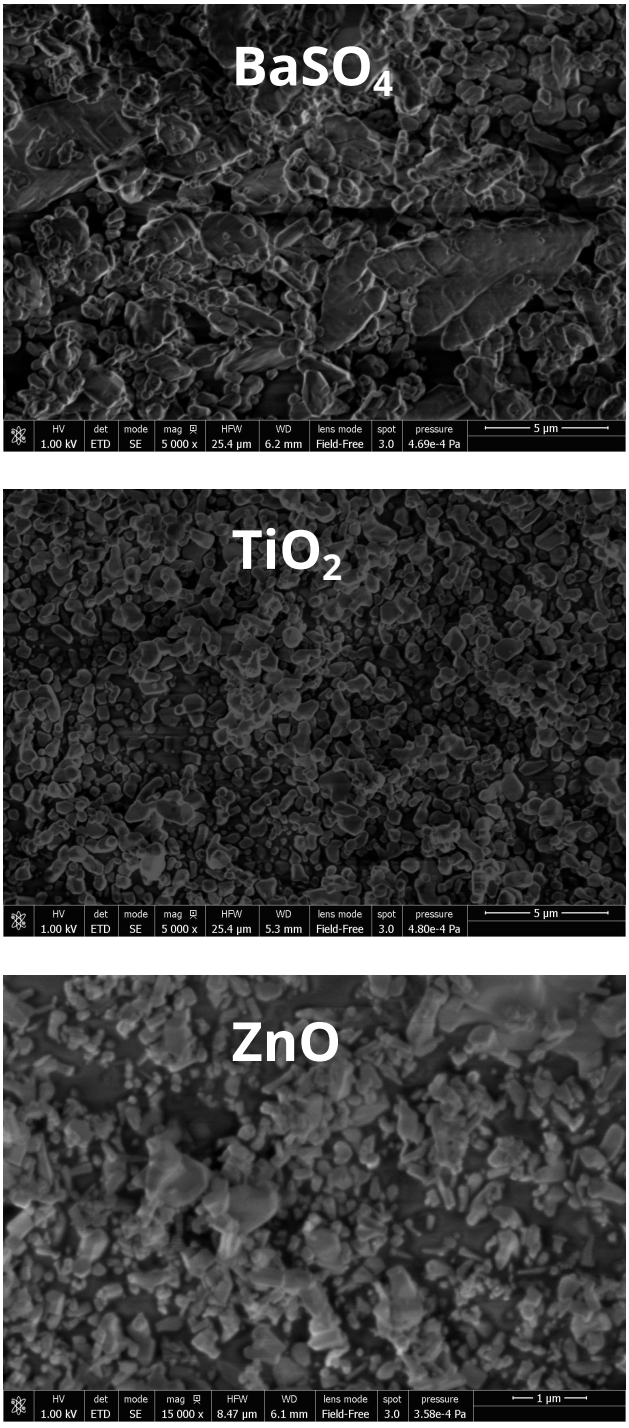

Figure A.4 SEM images of $BaSO_4$, TiO_2 and ZnO pigments. $BaSO_4$ shows a more heterogeneous size distribution compared to TiO_2 but in the same 1–5 μm range, ZnO is smaller ($\approx$ 0.5 μm).

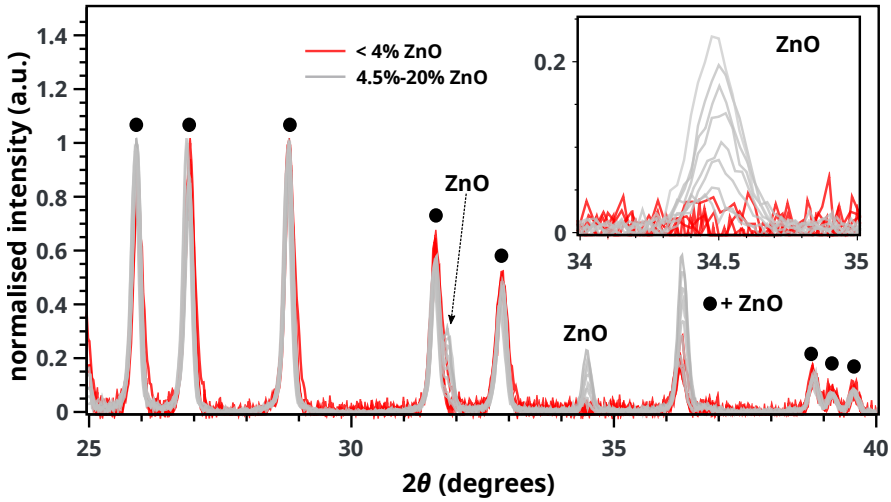

Figure A.5 $BaSO_4$ normalised XRD spectra for ZnO/$BaSO_4$ paints containing 0.5–20 wt % of ZnO. Inset shows that ZnO is completely consumed below ≈ 4.5 wt%. $BaSO_4$ peaks are marked with ●.

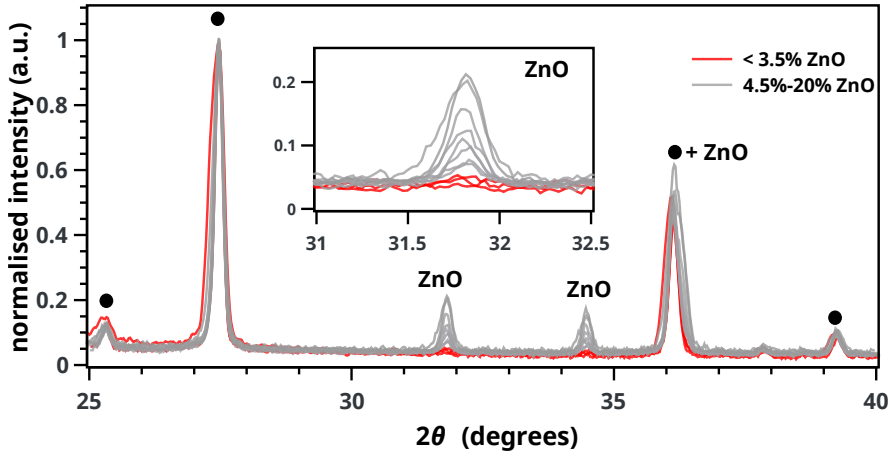

Figure A.6 TiO_2 normalised XRD spectra for ZnO/TiO_2 paints containing 0.5–20 wt % of ZnO. Inset shows that ZnO is fully consumed below ≈ 4.5 wt%. TiO_2 peaks are marked with ●.